Advances in Redox Research 9 (2023) 100081

Contents lists available at ScienceDirect

Advances in Redox Research

journal homepage: www.elsevier.com/locate/arres

Full Length Article

Regulation of metabolism, stress response, and sod1 activity by cytosolic thioredoxins in yeast depends on growth phase

Cecilia Picazo [a,*], C. Alicia Padilla [b,c], Brian McDonagh [d], Emilia Matallana [a], José A. Bárcena [b,c], Agustín Aranda [a]

[a] Institute for Integrative Systems Biology, I2SysBio, University of Valencia-CSIC, 7, Paterna 46980, Spain
[b] Department of Biochemistry and Molecular Biology, University of Cordoba, Cordoba, Spain
[c] Maimonides Institute for Biomedical Research of Cordoba (IMIBIC), Cordoba, Spain
[d] Discipline of Physiology, School of Medicine, University of Galway, Ireland

ARTICLE INFO

Keywords:
Thioredoxins
Sod1
Oxidative stress
Thiol redox proteome

ABSTRACT

Reactive Oxygen Species (ROS) can be harmful compounds that can cause damage to macromolecules like lipids, proteins, and DNA when their levels exceed cellular defense mechanisms. Cells have protection and ROS detoxification systems, including thioredoxin and glutaredoxin systems, to counteract oxidative stress. The role of cytosolic thioredoxin system (cTRX) was investigated in different growth phases using a mutant strain lacking both *TRX1* and *TRX2*. The mutant showed a defect in survival during the non-dividing state or stationary phase. The levels of glutathione, an antioxidant, in the mutants were higher in both total and reduced glutathione, indicating an increase in oxidative response. The mutant also showed an increase in protein-bound glutathione, suggesting a compensatory mechanism to counter balance oxidative stress. Proteomic analysis revealed changes in the expression of various proteins in the absence of cytosolic thioredoxins. Upregulated proteins in both exponential and stationary phases were mainly related to oxidative stress response and metabolism. Down-regulated proteins in both phases were associated with glycerol metabolism, glycolysis, and ATP synthesis. These changes indicated a compensatory response to redox imbalance caused by the absence of cytosolic thioredoxins. Further analysis focused on the reversible oxidation of cysteine residues in proteins. Several proteins were identified with cysteines susceptible to reversible oxidation, and their oxidation status was affected by the absence of cytosolic thioredoxins. Notably, cysteine 146 of cytosolic Superoxide Dismutase 1 (Sod1) was more oxidized in growth phase, while oxidation of ribosomal proteins was seen only in exponential phase.

Overall, this study provides insights into the role of cytosolic thioredoxin system in growth, aging, in maintaining redox balance, protecting against oxidative stress as well as its impact on *SOD1* activity and glutathionylation.

Introduction

Reactive Oxygen Species (ROS) are cytotoxic compounds formed *in vivo* as a result of mitochondrial respiration and cause, when their levels overwhelm cellular defenses, damage to macromolecules as lipids, proteins and DNA [1]. To counteract oxidative stress, cells have protective and ROS detoxification mechanisms to prevent damage at the macromolecular level. Two pathways involve cysteine-thiol redox systems, which comprise thioredoxin and glutathione/glutaredoxin system [2]. Thioredoxins (TRX) are oxidoreductases with two cysteines in their active sites that are implicated in disulfide reduction. In *Saccharomyces cerevisiae*, cytoplasmatic thioredoxin system (cTRX) is formed by two thioredoxins, Trx1 and Trx2, and one thioredoxin reductase, Trr1, that provides reducing power from NADPH [3]. Their most important function is completing the catalytic cycles of interacting enzymes, like the thioredoxin-dependent peroxidases called peroxiredoxins. A mutant strain for both thioredoxins is auxotrophic for sulfur amino acids because thioredoxins provide the hydrogen group donor to 3′-phosphoadenosine-5′-phosphosulfate (PAPS) reductase, which converts PAPS into sulfide. Mutants also have a defect in S phase of the cellular cycle because thioredoxins are responsible for ribonucleotide reductase (RNR) reduction to keep RNR active [4,5]. Thioredoxins play a crucial role in

* Corresponding author.
E-mail address: cecilia.picazo@uv.es (C. Picazo).

https://doi.org/10.1016/j.arres.2023.100081
Received 12 July 2023; Received in revised form 5 September 2023; Accepted 12 September 2023
Available online 20 September 2023

regulating disulfide bonds between thiol groups in cysteine residues of proteins [3]. The thiol groups in cysteines are also susceptible to irreversible oxidation. Posttranslational modifications such as glutathionylation can protect thiols from irreversible oxidation [6,7]. The involvement of thioredoxin and glutaredoxin systems in the regulation of glutathionylation has been suggested, although this process remains poorly understood [8]. Grant et al. demonstrated that cTRX may play a role in deglutathionylation, removing the GSH bound to protein following oxidative stress [9]. Additionally, yeast mitochondrial Trx3 has been shown to deglutathionylate the peroxidatic Cys91 of the 1-Cys-mitochondrial peroxiredoxin Prx1 [10]. *S. cerevisiae* has five thioredoxin peroxidases also known as peroxiredoxins, which rely on the thioredoxin system to complete their catalytic cycle. Peroxiredoxins use cysteines in their active site to detoxify peroxides and they are classified as 1-Cys-or 2-Cys-peroxiredoxins. While 1-Cys-peroxiredoxins contain a peroxidatic Cys-residue, they lack a resolving Cys-residue found in 2-Cys-peroxiredoxins. In the presence of ROS, the thiol group (-SH) of the peroxidatic Cys-residue is oxidized to form a sulfenic (-SOH) that may, e.g., result in disulfide bond formation (-S-S-) or can be further oxidized to generate cysteine sulfinic ($-SO_2H$) and sulfonic ($-SO_3H$) acid forms.

Imbalances between ROS and the antioxidant defense mechanisms play a significant role in various conditions, including carcinogenesis, response to chemotherapy and age-related diseases such Parkinson's, Alzheimer's and Amyotrophic Lateral Sclerosis (ALS). ALS is a fatal neurodegenerative disease [11]. The etiology of ALS remains unclear and currently there are several proposed mechanisms for ALS pathogenesis. A portion of ALS cases (10 %) is inherited (familiar ALS o fALS) caused by mutation in specific genes. The first causative gene associated with ALS and extensively studied is superoxide dismutase 1 (SOD1), a Cu/Zn Sod1 antioxidant enzyme [12]. SOD1 is a Cu/Zn superoxide dismutase that catalyze the dismutation of superoxide into oxygen and H_2O_2. While human Sod1 contains four Cys-residues, its yeast homologue has two (Supplementary Fig. 1). The disulfide bound formed between Sod1 Cys 146 and Cys57 coordination histidine residues (His46, His48, His120 and His63) to metal cofactors (Cu and Zn), stabilizing the enzyme [13]. Oxidation of Zn ligand with loss of the metal or disruption of Cys57-Cys146 disulfide produces enzyme destabilization and promotes Sod1 aggregation (Martins & English, [14]). Research on yeast stationary cells, akin to quiescent motor neurons, demonstrated that Cys146 is oxidized and catalytically inactive, in contrast to reduced Cys57 [13]. This oxidation is critical for the folding and stability of Sod1. Furthermore, human tissues studies revealed substantial glutathionylation of Sod1 at Cysteine-111, profoundly affecting dimer stability [15]. Studies have implicated glutaredoxins, thioredoxins and thioredoxin reductase in Sod1 regulation and ALS (Hitchler & Domann., [16,17]).

In addition, the role of Sod1 extends beyond its antioxidant function. It has been described as a key metabolic regulator. In 2013, Reddi et al. showed that O_2, glucose and Sod1 cooperates to maintain the stability of Yck1 and Yck2, two kinases related with respiratory repression (Reddi & Culotta., [18]). Moreover, in 2014 Chi Kwan Tsang lab revealed that Sod1 localizes in the nucleus under H_2O_2 conditions, binding to DNA promoters and regulates gene expression important for resistance to oxidative DNA damage (Tsang et al., [19]).

In this study, we studied the role of cytosolic thioredoxin system during different growth phases, exponential and stationary. We demonstrated that the *trx1*Δ*trx2*Δ double mutant exhibits reduced survival in a non-dividing state or stationary phase, known as chronological life span (CLS), which is important for age-related disease. Through a global proteomic assay, we found a strong role of Trx1 and Trx2 in the oxidative stress response and in metabolism. By analyzing the thiol redox proteome, we revealed the role of Trx1 and Trx2 in regulating Sod1 activity and its glutathionylation, unknown until now. Notably, we found that cTRX system does not participate in Sod1 deglutathionylation.

Results

Impact of trx1Δtrx2Δ double mutant on growth and aging

In order to study the role of cytosolic thioredoxins on growth, mutants of *TRX1, TRX2* and the double mutant were tested in the haploid prototrophic yeast C9. Notably, there were no striking differences in growth in complete synthetic medium between the wild-type strain, the simple mutants and the *trx1*Δ*trx2*Δ double mutant (Fig. 1A). All mutants reached a similar maximum optical density (OD), indicating unimpaired growth. Interestingly, the double mutant had a reduced lag phase, suggesting a slightly better adaptation to fermentative growth. SC is the usual medium to perform Chronological Life Span (CLS) experiments, and accordingly, it was used to study the role of the double mutant in the survival in a non-dividing state (Fig. 1B). Both simple mutants exhibited survival rates similar to the wt-type strain. However, the *trx1*Δ*trx2*Δ double mutant viability decreased by day 2, plummeting to 1 % viability by day 7, whereas both the simple mutant and the wt-type strains maintained more than 10 % viability. These results indicate that the cytosolic thioredoxin (cTRX) system is not critical for cell growth in fermentative conditions but is important for cell survival in stationary phase where there is no division.

In the absence of cytosolic thioredoxins, the relevance of the glutathione system may become heightened as part of a compensatory mechanism. Levels of total glutathione, reduced GSH, and the ratio of between reduced to oxidized glutathione were assessed in the thioredoxin system mutants under different growth conditions, exponential and stationary phase, were measured (Fig. 1C). There were differences in intracellular GSH between growth phases. Exponential phase exhibited higher there were higher total, reduced GSH and oxidized GSSG levels compared to stationary phase in the wild type, indicating a higher biosynthetic metabolism. However, the GSH/GSSG ratio increased during stationary phase, suggesting adaptation to a more oxidative environmental. Single mutants showed a very similar profile, indicating that the system is robust and both thioredoxins are mainly redundant. Intriguingly, the levels of total and reduced glutathione were higher compared to the wt in the *trx1*Δ*trx2*Δ double mutant irrespective of growth phase, with a more pronounced difference observed during stationary phase (Fig 1C). Additionally, oxidized glutathione increased from the stationary phase and seem to be accumulated later in growth. These results indicate that the *trx1*Δ*trx2*Δ double mutant produces an increase in oxidative stress which the cell counter balances by increasing the GSH levels and subsequently an increase in GSSG.

One-way GSH exerts protection against oxidative stress is through glutathionylation, a reversible posttranslational modification. Protein-bound GSH was measured in all the strains and in both growth phases (Fig. 1D). Notably, no significant disparities in protein-bound GSH were observed between the wild-type strain and single mutants during both growth phases. However, the *trx1*Δ*trx2*Δ double mutant exhibited a significant increase in protein-bound GSH in stationary phase (Fig 1D). This might reflect the rise in overall glutathione in conditions of oxidative pressure and is coherent with higher oxidized glutathione. It also suggests that *TRX1* and *TRX2* may be important for deglutathionylation in stationary phase.

Upregulated proteins in the trx1Δtrx2Δ double mutant along growth

For a better understanding of the role of the cytosolic thioredoxin system across growth phases, a quantitative study of the differential proteome of wild-type strain and the *trx1*Δ*trx2*Δ double mutant was performed. In exponential phase in minimal medium, 69 proteins exhibited statistically significant quantitative changes (fold change above 1.5) between the *trx1*Δ*trx2*Δ double mutant and the wild-type strain (see Supplemental Material 3). During stationary phase, 149 proteins displayed statistically significant quantitative changes (Supplemental Table 4). Of these detected proteins, 99 were upregulated in

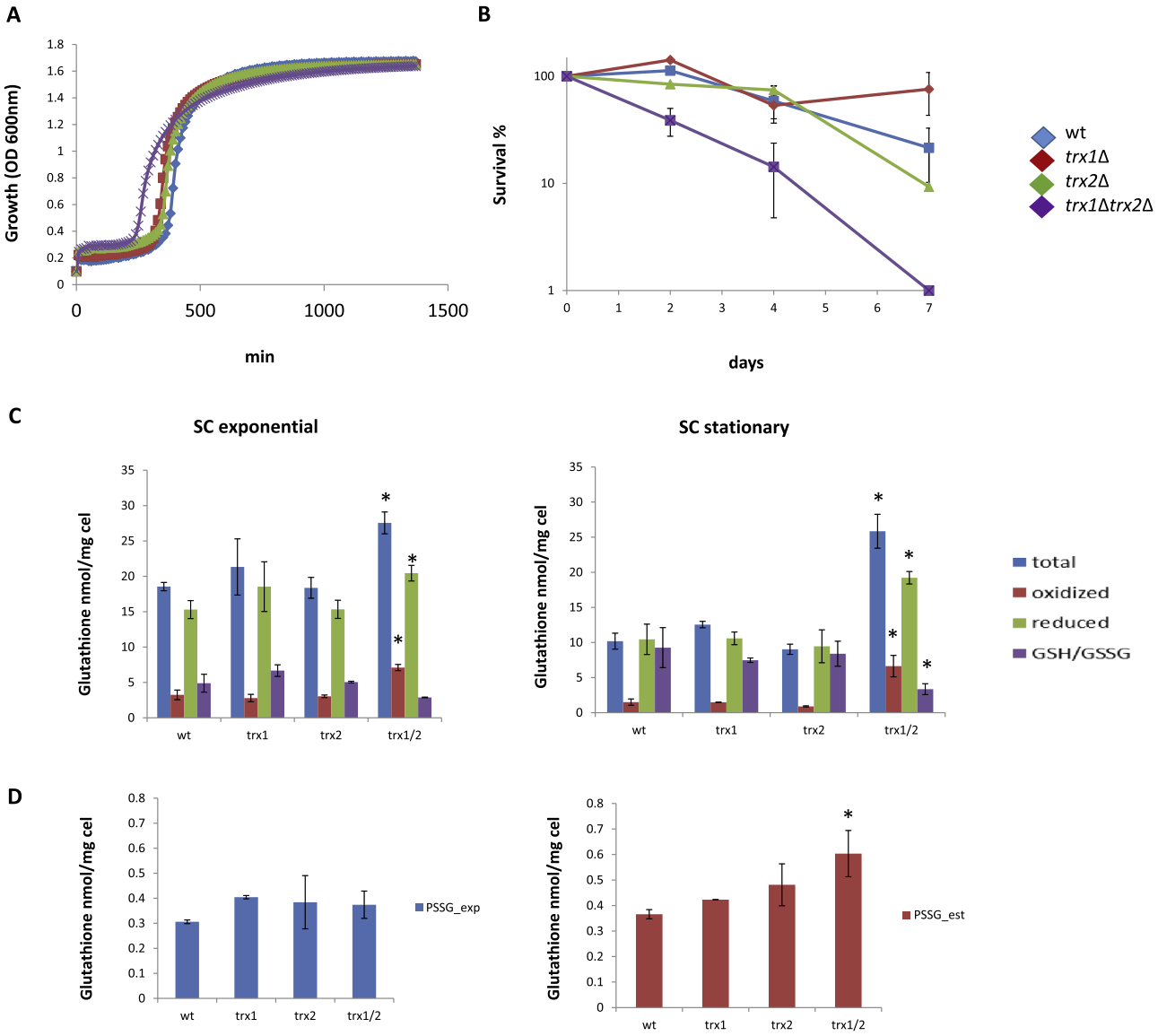

Fig. 1. *TRX1* and *TRX2* impact on growth and glutathione metabolism in Complete Synthetic Medium (SC). Growth curves profile (A). Survival curve after 3 days of growth in SC medium (B). Determination of glutathione levels in cells in exponential and stationary phase. Total, oxidized glutathione (GSSG), reduced glutathione (GSH) and GSH/GSSG ratio (C). Protein-bound glutathione assay (D). Experiments were done in triplicate. Means and standard deviations are provided. *$P<0.05$, unpaired *t*-test, two-tailed.

the *trx1*Δ*trx2*Δ double mutant. Functional categorization of upregulated proteins unique to exponential and stationary phases, as well as those common to both phases, was depicted using String [20] (Fig. 2A). Only nine were shared across both exponential and stationary phase. An interaction map based on these common proteins was used to identify enrichment in functional categories (Fig. 2A), as illustrated in Fig. 2B. Under "Biological Processes", the main enriched category was oxidative stress response, which is upregulated in both growth phases, including superoxide dismutase **Sod2**, thioredoxin reductase **Trr1**, oxidoreductase **Oye3**, and peroxidases **Ccp1** and **Gpx2**. These findings suggest that cells lacking the antioxidant proteins *TRX1* and *TRX2* increase the expression of other oxidative stress-related proteins as a compensation mechanism for survival. An impact in metabolism was also relevant, highlighted by the increase in Rnr4, Lys21, and Met17.

In the *trx1*Δ*trx2*Δ mutant there were nine other oxidative stress response-related proteins upregulated during the exponential phase (Fig. 2A). Notably, three of the five peroxiredoxins were augmented in the *trx1*Δ*trx2*Δ mutant during exponential phase, cytosolic peroxiredoxins **Tsa1** and **Ahp1** and the mitochondrial peroxiredoxin, **Prx1**. Moreover, sulfiredoxin 1 (**Srx1**), responsible for reversing hyperoxidation of Tsa1 [21], exhibited 32-fold increase abundant in the double mutant. A protein tag GFP was used to explore if the *trx1*Δ*trx2*Δ double mutant has a defect in Tsa1 aggregation (Supplemental Fig. 2) under different conditions (under H_2O_2 and AZC a proline analog that promotes protein aggregation). Green fluorescence intensity was higher in the *trx1*Δ*trx2*Δ mutant possibly attributed to increased Tsa1 concentration (2.1-fold) but there is still aggregation. Other proteins related with oxidative stress response were upregulated in *trx1*Δ*trx2*Δ mutant only in exponential phase: superoxide dismutase 1 (**Sod1**), methionine S-sulfoxide reductase (**Mxr1**), mitochondrial glutaredoxin (**Grx2**), glutathione reductase (**Glr1**) and cystathione gamma-lyase (**Cys3**). Exponential phase is a dividing state where cells have an active metabolism and need to deal with different stress, hence cells lacking the cTRX system necessitates the upregulation of alternative antioxidant defenses for compensation.

The second enriched biological category during exponential phase is related with lysine metabolism (Fig. 2A). Three of them belong to the lysine biosynthetic pathway, **Lys1, Lys9** and **Lys20** and the putative

A

UPREGULATED

Common Cellular response to oxidative stress			
Protein	Name	Fold Change Exponential	 Stationary
Met17	Protein MET17	1,6	2,3
Lys21	Mitochondrial homocitrate synthase	3,1	1,6
Rnr4	Ribonucleoside-diphosphate reductase	4,1	2,9
Sod2	Mitochondrial manganese superoxide dismutase	4,5	2,34
Trr1	Cytosolic thioredoxin reductase	6,6	5
Oye3	Conserved NADPH oxidoreductase containing flavin mononucleotide (FMN)	8,7	2
Cpp1	Mitocondrial cytochrome-c peroxidase	8,7	5
Gpx2	Glutathione peroxidase	10	3,3
Hbn1	Putative nitroreductase	11,4	4,1

Exponential Cellular response to oxidative stress			Lysine Metabolism		
Protein	Name	Fold Change	Protein	Name	Fold change
Mxr1	Methionine S-sulfoxide reductase	1,95	Lys9	Saccharopine dehydrogenase	2,84
Tsa1	Peroxiredoxin 1	2,1	Lys1	Saccharopine dehydrogenase	2,97
Glr1	Glutathione reductase	2,1	Lys20	Homocitrate synthase isozyme	3,13
Cys3	Cystathione gamma-lyase	2,2	Aco2	Putative mitochondrial aconitase isoenzyme	3,38
Sod1	Superoxide dismutase 1	2,33			
Grx2	Mitochondrial glutaredoxin	2,4			
Ahp1	Thiol-specific peroxiredoxin	3,28			
Prx1	Mitochondrial peroxiredoxin	4,45			
Srx1	Sulfiredoxin 1	32			

Stationary Carboxylic acid metabolism		
Protein	Name	Fold change
Cit2	Cytochrome c1 heme lyase	1,6
Cyb2	Cytochrome b2	1,61
Cit1	Citrate synthetase	1,7
Leu4	alpha-isopropylmalate synthase	1,7
Met5	sulfite reductase	1,7
Ymr31	37 ribosomal protein YMR-31	1,72
Acs2	acetyl-CoA synthetase	1,8
Asn2	Asparagine synthetase	1,98

B

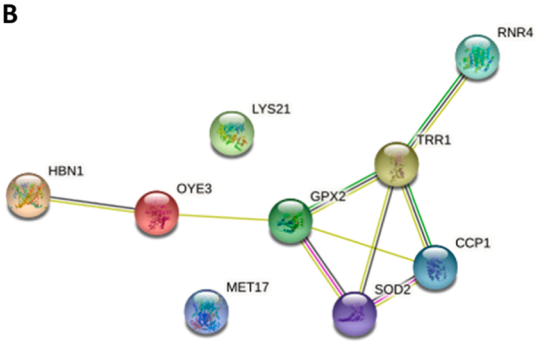

Fig. 2. *TRX1* and *TRX2* deletion impacts on metabolism depending on growth conditions. Functional analysis of the abundance of proteins stadistically significant upregulated enriched in *trx1*Δ*trx2*Δ mutant (A) and the interactome node base on the common proteins acording to String (B).

mitochondrial aconitase isoenzyme **Aco2** showed a 3-fold increase (Supplemental Material 3). Despite the overexpression of enzymes froma the upper lysine biosynthesis pathway in the *trx1*Δ*trx2*Δ double mutant resistance to thiolysine (S-2-aminoethyl-L-cysteine (AEC)), a toxic lysine analogue, remained unaffected (Supplementary Fig. 3). suggesting pathway activation stems from deficit rather than a protective mechanism.

In stationary phase, enrichment of the eight upregulated proteins point towards carboxylic acid metabolism (Fig. 2A). Carbon metabolism proteins (citrate synthetase, **Cit1**, acetyl-CoA synthetase, **Acs2**, Cytochrome c1, **Cit2**) and amino acid (alpha-isopropylmalate synthase, **Leu4** and **Met5**, sulfite reductase) exhibited increased levels. Noteworthy, two highly abundant proteins include **Isd11**, a cysteine desulfurase activator essential for the formation of the persulfide intermediate at the desulfurase active site during pyridoxal phosphatase- dependent desulfuration of cysteine which displayed a 27.6-fold increase in the double mutant compared to the wild type, and **Sno4** (83-fold) is a probable glutathione-independent glyoxalase, possible chaperone and cysteine protease, required for transcriptional reprogramming during the diauxic shift and for survival in stationary phase.

Downregulated proteins in the trx1Δtrx2Δ double mutant in exponential and stationary phases

Due to the impact of cTRX system on global proteome, proteins downregulated in the *trx1*Δ*trx2*Δ mutant were investigated (Fig. 3). A total of seven common downregulated proteins were identified, all of them belonging to the "response to stress" biological category according to String (Fig. 3A). Among these, three were related to glycerol metabolism, two glycerol-1-phosphatase, **Gpp1** and **Gpp2**, and a glycerol-2-dehydrogenase, **Gcy1**. These proteins exhibit functional connection with **Ctt1** a cytosolic catalase (Fig. 3B), that was also downregulated. Catalase activity was measured in the wt and in the *trx1*Δ*trx2*Δ mutant in both growth conditions (Fig 3C). There was an increase in catalase activity during the transition from exponential to stationary phase, and this increase remained consistent in both strains. However, the levels of

A

DOWNREGULATED

Common

Response to Stress

Protein	Name	Fold Change Exponential	Fold Change Stationary
Gpp1	Glycerol-1-phosphatase	0,4	0,29
Gpp2	Glycerol-1-phosphatase	0,23	0,3
Gcy1	Glycerol-2-dehydrogenase	0,04	0,38
Ctt1	Cytosolic catalase	0,2	0,14
Hsp26	Heat shock protein 26	0,22	0,38
Hta1	Histone H2A	0,49	0,24
Lsp1	Sphingolipid long chain base-responsive protein	0,47	0,42

Stationary

Cellular carbohydrate metabolism

Protein	Name	Fold Change
Pgm2	Phosphoglucomutase 2	0,26
Gas1	1,3-beta-glucanosyltransferase	0,28
Tps2	Trehalose-phosphatase	0,29
Glc3	1,4-alpha-glucan-branching enzyme	0,3
Dak1	Dihydroxyacetone kinase	0,32
Gph1	Glycogen phosphorylase	0,32
Ara1	D-arabinose dehydrogenase	0,33
Hxk1	Hexokinase-1	0,35
Hsp104	Heat shock protein 104	0,38
Tps1	alpha-trehalose-phosphate synthase	0,4
Idp1	Isocitrate dehydrogenase	0,46
Glk1	Glucokinase-1	0,47
Hxk2	Hexokinase-2	0,49

Nucleotide biosynthetic pathway

Protein	Name	Fold change
Atp14	ATP synthase subunit H	0,09
Atp7	ATP synthase subunit d	0,12
Tim11	ATP synthase subunit e	0,26
Cyt1	Cytochrome c1	0,27
Pma2	Plasma membrane ATPase 2	0,32
Apa1	Protein APA1	0,37
Pnc1	Nicotinamidase	0,39
Ade16	Bifunctional purine biosynthesis protein	0,41
Ade1	Phosphoribosylaminoimidazole-succinocarboxamide synthase	0,46
Atp3	ATP synthase subunit gamma	0,46
Atp16	ATP synthase subunit delta	0,47

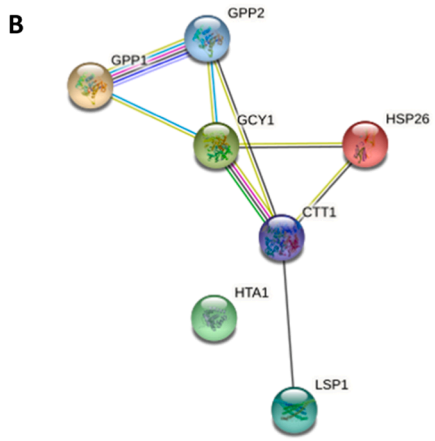

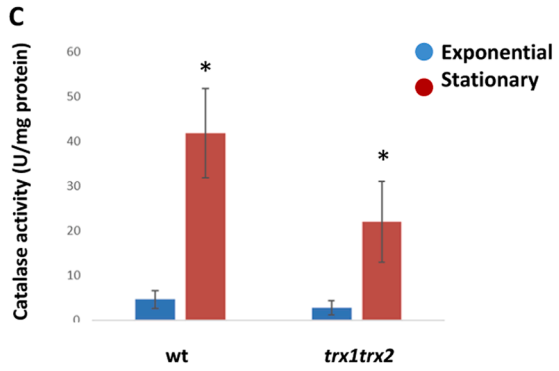

Fig. 3. *TRX1* and *TRX2* deletion impacts on metabolism depending on growth conditions. Functional analysis of the abundance of proteins stadistically significant downregulated (A) in *trx1*Δ*trx2*Δ mutant and the interactome node base on common proteins acording to String (B). Catalase activity in both growth phases are shown. Experiments were done in triplicate. Means and standard deviations are provided. *$P<0.05$, unpaired *t*-test, two-tailed (C).

catalase activity in the *trx1*Δ*trx2*Δ mutant were lower than in the wt in both growth phases accordance with the proteomic findings, implying an absence of compensatory mechanisms.

As demonstrated in Fig. 3A, only nine proteins were statistically significant downregulated in exponential phase, without a discernible enrichment in biological categories. However, during stationary phase, there were 116 proteins significantly downregulated. Enrich analysis revealed the "cellular carbohydrate metabolism" category, encompassing 13 proteins that could be categorized into two distinct groups. The first group is related to glycolysis and includes hexokinase **Hxk1** and **Hxk2** glucokinase, **Glk1** and phosphoglucomutase, **Pgm2**, involved in the first step of sugars phosphorylation. The second group pertains to carbohydrate protection: two subunits of the trehalose-6-phosphate synthetase complex, **Tps1** and **Tps2** and proteins of glycogen metabolism, glycogen phosphorylase **Gph1** and branching enzyme **Glc3**.

Another set of eleven downregulated proteins in stationary phase was clustered into the nucleotide biosynthetic pathway. One group is related with ATP synthesis and belong to ATP synthase complex **Atp3, Atp7, Atp14, Atp16, Tim11, Pma2** and **Cyt1**. Another group was related with purine biosynthesis, **Ade16** and **Ade1** (Fig. 3A).

Taken all together, all these proteomic alterations resulting from the removal of the cTRX system indicate that this system plays a crucial role for the correct redox balance in the cells. Moreover, glycolysis and ATP synthesis downregulation point to a compensatory mechanism to deal with a redox unbalance in the cell that eventually leads to lower survival rate.

Cytosolic thioredoxins influence in thiol reversible oxidation

Cysteine thiol groups within proteins can be reversibly oxidized as part of protective and regulatory mechanisms when cells are exposed to oxidative challenge. Consistent with this notion, we previously observed an increase in protein-bound glutathione in the *trx1*Δ*trx2*Δ double mutant as shown in Fig. 1D. To identify proteins affected by reversible Cys-redox changes we carried out a redox proteomic analysis in the *trx1*Δ*trx2*Δ double mutant, based on differential stable isotope labeling of reduced and oxidized cysteines as described in Materials and Methods section [22,23] (Fig. 4 and Supplementary Tables 1 and 2). Seven proteins were detected with cysteines susceptible to reversible oxidation, and their affected Cys-residues were mapped. The accession number, name of the protein, Cys-residue and ratio between reduced and oxidized cysteines are shown for both the wt and the double mutant in exponential and stationary phase (Fig. 4A). Four proteins identified mainly in exponential phase were ribosomal proteins, likely reflecting their abundance during active growth. Interestingly, Cys38 of RPS29A was more oxidized in wt than in the mutant while Cys38 of RPS29B displayed more oxidized in the mutant. This result necessitates further investigation, potentially related to redox-mediated control of protein biosynthesis in ribosomal proteins (Stöcker et al., 2018). Additionally, two proteins related to respiratory metabolism (mitochondrial prolyl isomerase CPR3, Cys57 and NADPH aldose reductase GRE3, Cys27) were solely identified in stationary phase. In the double mutant, one Cys-residue of each of these proteins was more oxidized in the mutant than in wt, as should be expected from the antioxidant weakness of the

A

Accession Number	Protein	Redox Cys	SC Exponential Ratio Red/oxi	SC Stationary Ratio Red/oxi
P00445	Superoxide dismutase [Cu-Zn] (SOD1)	Cys 146	wt 0,45	wt 0,3
			trx1trx2Δ 0,06	*trx1trx2Δ* 0,43
P41057	40S ribosomal protein S29-A (RPS29A)	Cys 38	wt 0,63	
			trx1trx2Δ 15,35	
P41058	40S ribosomal protein S29-B (RPS29B)	Cys 38	wt 2,37	
			trx1trx2Δ 0,39	
P41058	40S ribosomal protein S29-B (RPS29B)	Cys 23	wt 2,47	
			trx1trx2Δ 4,11	
P0C0W1	40S ribosomal protein S22-A (RPS22A)	Cys 71	wt 5,2	
			trx1trx2Δ 3,45	
P25719	Peptidyl-prolyl cis-trans isomerase C, mitochondrial (CPR3)	Cys 57		wt 20,5
				trx1trx2Δ 6
P38715	NADPH-dependent aldose reductase GRE3 (GRE3)	Cys 27		wt 1,84
				trx1trx2Δ 0,5
P0CX25	60S ribosomal protein L43-A (RPL43A)	Cys 38		wt 5,3
				trx1trx2Δ 3,6

B

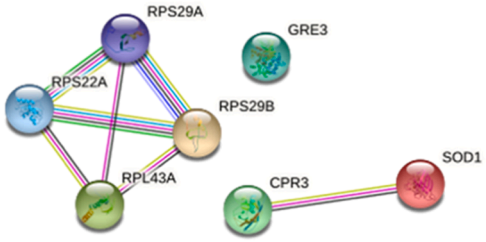

C

Biological Process (GO)

Pathway ID	Pathway description	Count in gene set	False Discovery rate
GO:0022626	Cytosolic ribosome	4	0,0105
GO:0044391	Ribosomal subunit	4	0,0164

Fig. 4. Impact of Trx1 and Trx2 on reversible oxidation. List of Proteins Containing Redox-Sensitive Cys-Residues Detected by the Redox Proteomic Approach in exponential and in stationary phase in the wild-type strain and in the *trx1*Δ*trx2*Δ double mutant. Accession number, protein name, redox cysteine and ratio between reduced and oxidized have shown. The redox state of selected redox Cys-residues labeled with both d(0) NEM and d(5) NEM was calculated using Skyline open software (A). Interactome node based on the proteins detected with oxidative reversible cysteines (B) and functional analysis of proteins from B (C).

*trx1*Δ*trx2*Δ mutant under these conditions.

Cys146 of cytosolic Superoxide Dismutase 1 (Sod1) was the only one detected in both growth phases and was deeply oxidized in the mutant in exponential phase with a ratio of reduced/oxidized Cys-of 0.06 but changed to 0.43 in stationary phase. In contrast, this ratio was roughly similar in both phases (0.45 and 0.30) in wt cells, indicating a further reduction in the mutant. Interestingly, Cys146 of Sod1 was mostly reduced in exponential phase when the cells grow in YPD medium (a rich medium with 2 % of glucose similar to SC medium), with ratios of 56.62 and 13.76 for wt and *trx1*Δ*trx2*Δ, respectively. Despite this, even under these conditions, the Sod1 Cys146 in the mutant did not reach the reductive level of wt (data not shown).

Cys146 forms an intramolecular disulfide bond with Cys57 to stabilize Sod1 dimer, and disruption of the disulfide promotes Sod1 aggregation [24]. Due to this important role of the disulfide bond, we sought to investigate whether the cTRX system function as a regulator of Sod1 activity. Notably, Human Sod1 contains four cysteine residues at positions 6, 57, 111 and 146. However, *S. cerevisiae* has only two, Cys 57 and Cys 146 (Supplemental Fig. 1). The tryptic peptide containing Cys57 was not detected in mass spectrometry analysis likely due to its large size (25 residues). We focused on the potential involvement of cTRX system in regulating the redox status of Cys146 and its impact on Sod1 activity.

SOD activity is dependent of cTRX system and sod1 is glutathionylated in a cTRX system independent manner

In order to study the role of cTRX system on SOD functionality, we checked the effect of *trx1*Δ*trx2*Δ double mutant on SOD activity and glutathionylation. SOD activity was measured using zymogram assay [25] (Fig. 5A) with *trr1*Δ and *tsa1*Δ mutants as a control strains. Notably, both the *trx1*Δ*trx2*Δ double mutant and *trr1*Δ mutant exhibited higher SOD activity than the wt and the *tsa1*Δ mutant, across both exponential and stationary growth conditions. Moreover, during exponential phase in YPD medium (a nutrient-rich medium), the *trx1*Δ*trx2*Δ double mutant displayed elevated SOD activity compare to the wt (Supplemental Fig. 4).

Previous studies have shown that oxidative stress (induced by H_2O_2) produces destabilization of Cys57-Cys146 disulfide bond and subsequent Sod1 aggregation (Chen et al., [26]; Nitesh et al., [27]). Furthermore, Sod1 has been implicated as a nuclear transcription factor under H_2O_2 conditions, regulating the expression of oxidative stress genes [19]. We treated yeast cells with the superoxide-generating agent 4-nitroquinoline-N-oxide (4NQO) to check if *trx1*Δ*trx2*Δ double mutant has a role in the nuclear localization of Sod1. However, there were no changes in Sod1 localization, compared to the wt (Fig. 5B).

In order to investigate the role of cTRX system in posttranslational modification, an immunoprecipitation assay using myc-tagged Sod1, following byWestern blot with anti-GSH antibodies were performed to check potential Sod1 glutathionylation under our conditions (Fig. 6). Previously, we have shown that the levels of GSH are higher in *trx1*Δ*trx2*Δ than in the wild-type strain in stationary phase, although the GSH/GSSG ratio is lower (Fig. 1C). We have checked the different fraction of the co-IP protocol (Supplemental Fig. 5A) with anti-GSH and anti-MYC in the wt, *trx1*Δ*trx2*Δ double mutant and a strain without myc tag as a control (referred to as Mock). Our findings indicated the presence of GSH binding to Sod1 across all of the fractions and in both wt and *trx1*Δ*trx2*Δ double mutant. Interestingly, the *trx1*Δ*trx2*Δ double mutant has more levels of Sod1 protein in these conditions (as evident in

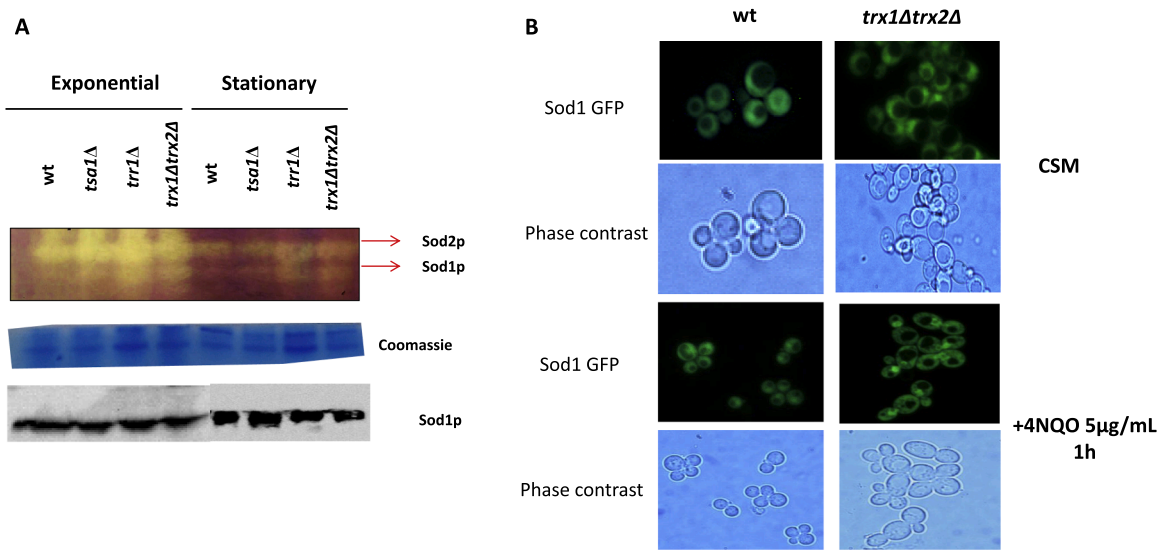

Fig. 5. cTRX system has an impact in SOD activity. Zymogram for the study of SOD activity in exponential and in stationary phase in SC medium in the wild-type strain, *trx1Δtrx2Δ* double mutant and *tsa1Δ* and *trr1Δ* as a control strains. Coomassie of the zymogram gel and western blot of Sod1 protein levels was showed as a loading control (A). Cells were treated with 5 µg/mL 4NQO during 1 h and analysed for Sod1-GFP localization by fluorescence microscopy in the wild-type strain and in the *trx1Δtrx2Δ* double mutant (B).

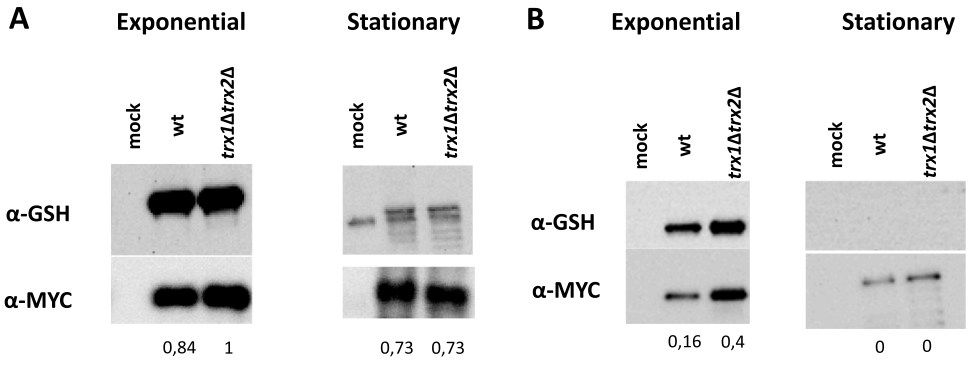

Fig. 6. Sod1 glutathionylation. Sod1-MYC immunoprecipitation in exponential and stationary phase in non-reducing conditions (A) and reducing conditions with 1 mM DTT (B) of the wt strain, *trx1Δtrx2Δ* double mutant and mock as a control.

the anti-MYC western blot). Moreover, we have studied the gluthationylation under oxidative stress conditions with H_2O_2 and using DTT as a reductor to break the bond between Sod1 and GSH (Supplemental Fig. 5B). There is more GSH binding to Sod1 in the *trx1Δtrx2Δ* double mutant than in the wt but it is not depended on stress conditions.

Coimmunoprecipitation assay were conducted under non-reducing condition during both exponential and stationary phases (Fig. 6A), as well as under reducing condition with DTT 1 mM to disrupt the bond between GSH and Sod1 (Fig. 6B). In the exponential phase, there is GSH bound to Sod1 but is not dependent on the cTRX system. Moreover, GSH was bound to Sod1 in stationary phase in an cTRX system independent way. In exponential phase, there is more GSH linked to Sod1 than in stationary phase, indicating it depends on the growth status. Collectively, these results suggest that GSH binding to Sod1 serves as a protective mechanism against oxidation, particularly crucial during the exponential phase in comparison to the stationary phase. However, our results cannot establish that cTRX system has a role in this particular function.

Discussion

Cytosolic thioredoxins are small proteins involved in multiple processes and function as protecting molecules against oxidative stress [3] due to their involvement in the reduction of the catalytic cycle of peroxiredoxins (among other proteins), pivotal proteins in stress response and aging [21].This work analyzed the impact of cytosolic thioredoxin system on growth phases, exponential and stationary phase in Complete Synthetic Medium (CSM or SC). During growth in CSM, the *trx1Δtrx2Δ* double mutant displayed similar growth than the wild type and the simple mutants (Fig. 1A). However, *trx1Δtrx2Δ* double mutant has a decreased chronological life span (CLS) (Fig. 1B). In CSM, containing 2 % glucose similar to the nutrient-rich YPD medium, glucose is consumed in a fermentative metabolism during initial growth hours, followed by a diauxic shift to respiratory metabolism upon sugar depletion. CLS is the viability of cells to survive in non-dividing state, which in CSM corresponds to sugar depletion around day 3 of growth [28,29]. Our findings indicate that the cytosolic thioredoxin system (cTRX) is necessary for survival during this non-diving state, when metabolism is respiratory. These are typical defects produced by mutations in antioxidant enzymes and cTRX system deletion trigger compensatory mechanisms, e.g. an increase in total and reduce glutathione (GSH) in both growth phases (Fig 1C). Our data suggest that cTRX system has an important role in the maintenance of GSH levels. In 2003, Grant et al., previously proposed a potential role of cTRX system in deglutathionylation, a posttranslational modification that protect proteins from irreversible oxidation. Levels of GSH linked to proteins were measure (Fig. 1D) revealing elevated GSH

binding to proteins in the trx1Δtrx2Δ double mutant during stationary phase. This finding supports the hypothesis that the cTRX system participates in deglutathionylation. Previous studies in our lab also indicates that absence of thioredoxin reductase triggers compensatory responses to oxidative stress. Lacking Trr1 yeast has a decrease in CLS and increase in antioxidants proteins (e.g., Tsa1), increase in GSH total and catalase activity [30]. Similar behavior was observed in the double thioredoxin mutant under winemaking conditions. In a grape Juice medium with higher sugar content (200 g/L), the cTRX system exhibited delayed and an extended CLS. This effect on growth rate is attribute to the effect of the *trx1*Δ*trx2*Δ double mutant in the initial steps of the glycolysis, specifically hexoses phosphorylation. Downregulation of Hxk1, Hxk2, and Glk1 during winemaking conditions led to altered glycolytic flux, as previously described [31].

The most obvious effect of thioredoxin 1 and 2 deletion was the upregulation of antioxidant proteins, a response observed across various growth media (Fig. 2A, B). Notably, five key proteins in the oxidative stress response were upregulated. The cytosolic thioredoxin reductase, Trr1, responsible for restoring the reduced status of both thioredoxins, exhibited a 6.6-fold increase in exponential phase and 5-fold in stationary. Interestingly, the mitochondrial thioredoxin system was not activated, implying that Trr1 may be providing redox potential to unknown donors. Glutaredoxins are the other redox-control mechanism in the cytosol. Glutathione peroxidase Gpx2 was 10 times more abundant in exponential phase and a 3.3-fold increase in stationary, which its expression being induced by oxidative stress in a Yap1 and Skn7-dependent manner. Moreover, in 2005, Tanaka et al., showed that Gpx2 is an atypical 2-cys peroxiredoxin using the thioredoxin system as an electron donor and recently, it was shown the role of Gpx2 in CLS through mitochondrial function [32]. Other oxidative stress-related proteins upregulated in a non-depend growth phase include Sod2, Oye3 and Ccp1. This data corroborates that in the *trx1*Δ*trx2*Δ double mutant there is an activation of a compensation mechanism. Notably, glycerol metabolism is the enriched biological category in the proteins downregulated in *trx1*Δ*trx2*Δ double mutant common in both phases, indicating a response to hyperosmotic stress that may be linked to thioredoxins or the NAD+/NADH balance.

In addition, Trx1 and Trx2 regulate the proteome in a growth condition dependent manner. During exponential phase, where cells are dividing, the cTRX system plays a pivotal role. One biological category specifically upregulated in exponential phase in the *trx1*Δ*trx2*Δ double mutant is related with oxidative stress response.

Among the five peroxiredoxins in *S. cerevisiae*, three are upregulated only in this growth phase. Tsa1, peroxiredoxin that is considered as a gerontogen and a redox sensor protein [33], exhibited 2.1-fold increased, although its aggregation was not dependent on the cTRX system (Supplem. Fig. 2). Ahp1 and Prx1 were 3.28-fold and 4.45-fold upregulated respectively. Moreover, Srx1, responsible for the reduction of peroxiredoxin sulfinic acid, showed a 32-fold increase. The importance of cTRX system in cells redox balance was demonstrated, in stationary phase, the double mutant had an increase in the abundance of key proteins of GSH metabolism, Isd11 (27.6-fold) and Sno4 (83-fold) that are necessary for the sulfide bond formations and for the transcriptional reprogramming after diauxic shift and survival in stationary phase. These findings reinforce the elevated intracellular GSH levels in the double mutant dutring stationary phase (Fig. 1C, D).

The cTRX system serves as the electron donor of peroxiredoxins. In its absence, there is an increase of these proteins to compensate the levels of intracellular oxidative stress, particularly pronounced during active metabolic phases. In addition, lysine biosynthesis metabolism is upregulated too. Lysine is an essential amino acid and has a tightly regulation [34]. First enzyme pathway, homocitrate synthase (HCS) coding by *LYS20* and *LYS21*, is the target of the feedback regulation and is strongly inhibited by L-lysine. Five main proteins in this pathway Lys 1, Lys 9, Aco2, Lys 20 and Lys 21 (this one is upregulated in stationary phase too) are 2.96, 2.84, 3.38, 3.13 and 3 times respectively more abundant in the trx1Δtrx2Δ double mutant and this increase is not related with higher amount of intracellular lysine (Supplem. Fig. 3). Moreover, in 2014, P.J. ODoherty et al. demonstrated an upregulation of lysine biosynthesis genes in response to oxidative stress induced by linoleic acid hydroperoxide.

Surprisingly, in our study we only detected proteins downregulated in *trx1*Δ*trx2*Δ double mutant in stationary phase. This group included proteins related to hexose metabolism and glycolysis. We have previously described the role of cTRX system during wine yeast biomass propagation [35,36] and, particularly, in hexoses metabolism [31,37]. Specifically, during grape juice fermentations, *TRX1* and *TRX2* regulate the initials steps in glycolysis pathway at the levels of hexoses phosphorylation. There was a downregulation in Hxk1, Hxk2 and Glk1. Metabolomic analysis confirmed alterations in glycolytic intermediates, with lower glucose-6-phosphate and higher fructose-6-phosphate and pyruvate levels in the trx1Δtrx2Δ double mutant during grape juice fermentation [31]. It seems that this regulation of cTRX system on glycolysis is more pronounced in stationary phase. In this work, we have shown that there is less abundance of Hxk1, Hxk2 and Glk1 and in the trehalose assimilation and glycogen metabolism. This downregulation of glycolysis could be explained by the fact that part of the energy involved in the glycolysis is redirected through pentose phosphate pathway (PPP) that is closely interconnected with glycolysis pathway. This redirection of the metabolic flux from glycolysis to the PPP can alter the redox equilibrium of the cytoplasmatic NADP(H) pool which provides the redox power for antioxidant systems [38]. For example, it has been known that in response to oxidant treatments, the glycolytic enzyme glyceraldehyde-3-phosphate dehydrogenase (GADPH) is inactivated and transported into the nucleus of the cell and has been found S-nitrosylated, S-thiolated, S-glutathionylated in numerous organisms [39]. Moreover, proteins implicated in PPP are induced under oxidative stress conditions. Cells with an increase influx to the PPP have a higher ratio of NADPH/NADP+ and have more resistance to oxidants [40].

We are aware that ROS cause a shift of the cellular redox state, resulting in alterations in the balance of NADH/NAD+ and NADPH/NADP+. The absence of cytoplasmatic thioredoxin can produce a regulation of glycolysis and PPP, leading to imbalance of redox state of the cell and the activation of compensation mechanisms as increase antioxidant proteins, lysine metabolism, glutathione metabolism and glycerol metabolism and decrease the glycolytic flux. *gpp1*Δ*gpp2*Δ double mutant produces small amount of glycerol and is hypersensitive to the superoxide anion generator, paraquat [41].

Moreover, in the line with this conclusion, we have shown that ATP synthesis is downregulated in the *trx1*Δ*trx2*Δ double mutant in stationary phase. Specifically, seven proteins related with ATP synthase complex are downregulated: Atp3 (0.46-fold), Atp7 (0.12-fold), Atp14 (0.09-fold), Atp16 (0.47-fold), Tim11 (0.26-fold), Pma2 (0.32-fold) and Cyt1 (0.27-fold).

Due to this important function, we studied the role of cTRX system on reversible oxidation cysteines using a thiol redox proteome assay. We have detected reversible oxidation of cysteines of proteins that are depend on cTRX system. One interested result is that cysteine 146 of Superoxide Dismutase 1 (Sod1) is redox regulated by the cTRX system. *SOD1* is a Cu/Zn superoxide dismutase that catalyze the dismutation of superoxide into oxygen and H_2O_2. Sod1 has been extensively studied since its misfolding and aggregation are associated with the development of neurodegenerative disease such as Amyotrophic Lateral Sclerosis (ALS), Parkinson's and Alzheimer (Cys146-SO_3H was isolated from Parkinson's and Alzheimer's brains). As we mentioned in the introduction one part of ALS (10 %) is inherited (familiar ALS o fALS) caused by mutation in specific genes. Increase oxidative stress has been associated with both fALS and ALS by increasing protein oxidation. In 2011, Redler et al. showed that Cys-111 of SOD1 glutathionylation induces structural rearrangements which regulate the stability of the wt [15]. *SOD1* of *Saccharomyces cerevisiae* there are only two cysteines (Cys57 and Cys 146) but not Cys 111 (Supplem. Fig. 1).

In our results from the thiol redox proteome assay we discovered that Cys146 of Sod1 is reversible oxidized in a growth phase dependent manner (Fig. 4) and that Sod1 is glutathionylated in our conditions in an independent *TRX1* and *TRX2* way (Fig. 6). We have shown that in the *trx1*Δ*trx2*Δ double mutant there are more *SOD1* activity than in the wt (Fig. 5A). This higher SOD activity and glutathionylation is not related with the role of Sod1 as a transcription factor (Fig. 5B). This work shows a new role of cTRX system on metabolism regulation depend on growth conditions. Moreover, tolerance of eukaryotic cells to oxidative stress may result in the identification of proteins that can work as therapeutic targets as metabolism proteins and a possible target against age related neurodegenerative diseases.

Materials and methods

Yeast strains, growth media and chronological life span measurement

The yeast strains used in this work derive from C9 haploid strain [42]. To perform gene disruptions, recyclable selection marker *loxP--kanMX-loxP* was amplified from plasmid pUG6 [43]. For multiple deletions recombinase *cre* under an inducible *GAL* promoter [44] were used to excise the *kanMX* marker. GFP tagging of Sod1 was made using plasmid pFA6-GFP-KanMX6 and MYC tagging of Sod1 for immunoprecipitation was made using plasmid pFA6a-13Myc-KanMX6 [45]. Yeasts were usually grown in rich YPD medium (1 % yeast extract, 2 % bactopeptone, 2 % glucose). Solid plates contained 2 % agar, and 20 μg mL^{-1} geneticin if required. SC medium contained 0.17 % yeast nitrogen base, 0.5 % ammonium sulfate, 2 % glucose and 0.2 % drop-out mix with all the amino acids [46]. For spot test, SD medium (contained 0.17 % yeast nitrogen base, 0.5 % ammonium sulfate and 2 % glucose) was used and 35 mg/L of AEC was added. Cycloheximide was used on SD plates at 1 μg/mL.

For the CLS experiments, precultures of selected strains were grown overnight on YPD and were then inoculated in SC media at an OD_{600} of 0.1. After 3 days of growth at 30 °C, aliquots were taken, diluted and plated. Colonies were counted and the percentage of survival was calculated by taking day 3 of growth as 100 % survival [29].

Glutathione determination

For the oxidized and total glutathione, supernatant extracts were obtained from 100 mg of cells and were used for glutathione determination by the method of glutathione reductase [47] and [48]. For the glutathione linked to proteins, pellet extracts were employed and glutathione was measure as described in [49], but adapting to our growth conditions. The amount of glutathione was expressed as nmol/mg of cells.

Co-inmunoprecipitation and western blot

For western blotting, cells were taken and broken with one volume of glass beads in a buffer containing Tris–HCl 0.1 M pH 7.5, NaCl 0.5 M, $MgCl_2$ 0.1 M, NP40 1 % (v/v), PMSF 10 mM and protease inhibitors (complete Mini, EDTA-free from Roche). Protein concentration was measured by the Bradford method using the Bio-Rad Protein assay following the manufacturer's instructions. Samples were diluted in loading buffer for SDS-PAGE (Tris–HCl 240 mM pH 6.8, SDS 8 % (p/v), glycerol 40 %, β-mercaptoethanol 10 %). After electrophoresis with an Invitrogen mini-gel device, the gel was blotted onto PVDF membranes with a semy-dry device (Invitrogen) for the Western blot analysis. Membranes were incubated overnight with the primary antibody at 4°. The ECL Western blotting detection system (Amersham) was used following the manufacturer's instructions. The anti-GSH antibody was obtained from Virogen (101-A), anti- Sod1 was obtained from Chemicon (AB5482) and the anti-MYC antibody was obtained from Santa Cruz Biotechnology (9E10: sc-40).

For Immunoprecipitation, cells from 50 mL/sample of mid-exponential phase YPD culture was pelleted, the pellet was washed with cold water and pelleted again, washed with 1 mL lysis buffer (50 mM Tris–HCl pH 8.0, 150 mM NaCl, 1 mM EDTA, 10 % Glycerol, 5 mM MgCl2 and protease-inhibitor cocktail). Cells were broken in 0.35 mL lysis buffer by beads at 4 °C in a FastPrep®−24. The extract was pelleted at 12,500 rpm at 4 °C and the supernatant was used for subsequent analyses. Three aliquots were taken for analysis: one for input protein levels, one of non-retention fraction and one of immunoprecipitation part. Anti-Myc Beads (anti-c-myc agarose affinity gel antibody, Sigma A7470) were prewashed with lysis-buffer (100 mL) before being pelleted by centrifugation at 1000 rpm, 1 min, washed three times with lysis buffer and boiled at 95 °C, 5 min with loading buffer for SDS-PAGE.

Proteomic analysis

Three cultures of C9 and C9 *trx1*Δ*trx2*Δ were grown in complete synthetic medium, which were taken in the exponential and in stationary phase. We followed the protocol described by [22,23]. For the proteome global analysis, cells were harvested and the pellet was washed twice with water and redissolved in lysis buffer (8 m urea, 100 mm NEM, 50 mm Tris-Cl, 2 mm EDTA, 0.1 % (v/v) Triton X-100, and 2 mm PMSF, pH 8.0) containing washed sea sand. Cells were obtained through cryogenic homogenization with liquid nitrogen. Samples were centrifuged at 15,000 × for 10 min at 4 °C to obtain the protein extract. Three independent cultures were used per strain. Samples were analyzed by liquid chromatography and mass spectroscopy (LC-MS/MS). The LTQ Orbitrap operated in the parallel mode with a resolution setting at 30, 000 of width at half height within the 400–1500 *m/z* range, followed by five collision-induced dissociations activated MS/MS in the DDA mode ("data-dependent acquisition mode") to select the most abundant masses. The maximum injection times for MS and MS/MS were 500 ms and 50 ms, respectively. Monoisotopic precursors were selected by excluding the species with charge +1, and normalized collision energies of 35 % for CID ("collision induced dissociation") were used. The minimum intensity threshold for MS/MS was 1000 accounts. MS/MS spectra were analyzed with the SEQUEST search engine against Uniprot database of *S. cerevisiae* (www.uniprot.org). We used the software for quantification "label-free" Progenesis QI for Proteomics (Non-Linear Dynamics, Waters) using the digital image files that contained all the data of the image captured by the sensor (RAW). The peptide signals represented in the retention time versus the *m/z* ratio were aligned and quantified from the "area under the curve" (AUC) to produce a list of peaks, which were grouped and identified with the Proteome Discoverer search engine (v 1.4) against the UniProt database.

For the thiol redox proteome, it was used the differential cysteine labeling with d(0)NEM and d(5)NEM ([22] and [23]) for the selection of peptides with a thiol group susceptible of reversible oxidation. Protein extracts for redox analysis were extracted in the presence of thiol blocking buffer containing d(0) NEM. Protein extracts for redox analysis were desalted using Zeba spin desalting columns (Thermo Scientific, Hemel, Hempstead, UK). Two hundred micrograms of the desalted protein extract was diluted up to 160 μL with 25 mM ammonium bicarbonate and denatured by addition of 10 μL of 1 % w/v RapiGest (Waters, Manchester, UK) in 25 mM ammonium bicarbonate and followed by incubation at 80 °C for 10 min. Reversibly oxidized Cys-residues were reduced by the addition of 10 μL of 100 mM TCEP and incubated at 60 °C for 10 min. Cys-residues that were reduced at this stage were subsequently alkylated with 10 μL of 200 mM d(5) NEM and incubated at room temperature for 30 min. 2 μg of trypsin (Sigma, Poole, UK) was added to the samples followed by incubation overnight at 37 °C. Cys-containing peptides detected independently with the same amino acid sequence with both d(0) NEM and d(5) NEM modification, with a p-value equivalent of 0.01 were considered "redox peptides". With all these redox peptides, a list was developed for targeted analysis using *m/z* data, retention times, and fragmentation spectra with open-source

Skyline software [50]. This analysis allowed to calculate the "reduced / oxidized" ratio (d (0)/d (5) NEM) of each Cys-from the intensities of each individual parental ion (Supplemental Table 1 and 2). Free software such as STRING (http://stringdb.org/cgi/network.pl) was used to view the functional group enrichments of each of the experiments, and VENNY (http://bioinfogp.cnb.csic.es/tools/venny /) for obtaining Venn diagrams.

Superoxide dismutase zymogram analysis and catalase activity

Cell samples (50 mg) were collected at exponential and stationary phase for protein extraction. Cells were resuspended in 500 μl extraction buffer (0.05 M Tris–HCl pH 8.5), a cocktail of protease inhibitors 1X (Roche, Switzerland) and 0.4 g of glass beads. Cells were broken in a FastPrep®−24 at 5.0 m s^{-1} for 30 s twice. Protein samples were separated by 10 % native acrylamide gel electrophoresis (running buffer: 3.03 g l^{-1} Tris, 14.41 g l^{-1} glycine) for 2 h at 15 mA and at 4 °C. Next, gel was immersed in a SOD-staining solution: 0.05 M Tris–HCl pH 8.0, 0.125 mg ml^{-1} MTT 3-(4–5(dimethylthiazol-2-yl)2–5-diphenyltetrazolium bromide, 0.07 mg ml^{-1} phenazine methosulphate (PMS) and 0.18 mg ml^{-1} $MgCl_2$. Gels were then exposed to sunlight for 5–10 min to visualize the corresponding SOD white bands on a orange background [51].

For catalase activity, extracts were obtained from 50 mg of cells and assayed spectrophotometrically as described by Jakuboswski (Jakuboswski et al., [52]). Enzyme activity was calculated using an extinction coefficient of 43,66 M–1cm–1 for H_2O_2 and catalase activity was expressed as μmol of H_2O_2 min–1 mg of protein–1 (U/mg prot) (Gamero-Sandemetrio et al., [25]).

Microscopy

The GFP-labeled cells were directly observed in the complete synthetic medium. For Tsa1- GFP aggregation cells were treated with hydrogen peroxide (H_2O_2) 0.6 mM and L-Azetidine–carboxylic acid (AZC, A0760 Merck) 5 mM. For Sod1 nuclear localization, cells were treated with 5 μg/mL 4-Nitroquinoline N-oxide (4NQO, N8141 Merck) for 1 h. Cells were visualized with the right filter under a Nikon Eclipse 90i fluorescence microscope.

Funding

Grant PID2021–122370OB-I00 to EM and AA funded by MCIN/AEI/10.13039/501,100,011,033 and by the European Union FEDER program. CP is supported by Maria Zambrano postdoc contract (ZA21–068) of Spanish Ministry of Universities and European COST Actions (CA21154): TRANSLACORE. JAB and CAP was financed by grants from the Spanish Ministry of Economy and Competitiveness (BFU2012–32056) and the Andalusian Government (Consejería de Economía, Innovación, Ciencia y Empleo, BIO-0216 and Grant PY20_00423).

CRediT authorship contribution statement

Cecilia Picazo: Conceptualization, Investigation, Formal analysis, Resources, Formal analysis, Writing – original draft. **C. Alicia Padilla:** Formal analysis. **Brian McDonagh:** Conceptualization, Investigation, Resources, Formal analysis. **Emilia Matallana:** Conceptualization, Investigation. **José A. Bárcena:** Conceptualization, Investigation, Resources, Formal analysis. **Agustín Aranda:** Investigation, Resources, Formal analysis, Writing – original draft.

Declaration of Competing Interest

The authors declare that they have no known competing financial interests or personal relationships that could have appeared to influence the work reported in this paper.

Data availability

I have share the link to my data/code at the attach file step.

Supplementary materials

Supplementary material associated with this article can be found, in the online version, at doi:10.1016/j.arres.2023.100081.

References

[1] K.A. Morano, C.M. Grant, W.S. Moye-Rowley, The response to heat shock and oxidative stress in Saccharomyces cerevisiae, Rev. Genet. 190 (4) (2012) 1157–1195, https://doi.org/10.1534/genetics.111.128033.
[2] C. Picazo, M. Molin, Impact of hydrogen peroxide on protein synthesis in yeast, Antioxidants 10 (Issue 6) (2021), https://doi.org/10.3390/antiox10060952. Vol. MDPI.
[3] E. Herrero, J. Ros, G. Bellí, E. Cabiscol, Redox control and oxidative stress in yeast cells, Biochim. Biophys. Acta 1780 (2008) 1217–1235, https://doi.org/10.1016/j.bbagen.2007.12.004.
[4] A. Koç, L.J. Wheeler, C.K. Mathews, G.F. Merrill, Replication-independent MCB gene induction and deoxyribonucleotide accumulation at G1/S in Saccharomyces cerevisiae, J. Biol. Chem. 278 (11) (2003) 9345–9352, https://doi.org/10.1074/jbc.M213013200.
[5] E.G.D. Muller, Thioredoxin deficiency in yeast prolongs S phase and shortens the G1 interval of the cell cycle, J. Biol. Chem. 266 (14) (1991) 9194–9202.
[6] J.J. Mieyal, P.B. Chock, Posttranslational modification of cysteine in redox signaling and oxidative stress: focus on s-glutathionylation, Antioxid. Redox Signal. 16 (6) (2012) 471–475, https://doi.org/10.1089/ars.2011.4454.
[7] M.J. Penninckx, An overview on glutathione in Saccharomyces versus non-conventional yeasts, FEMS Yeast Res. 2 (3) (2002) 295–305, https://doi.org/10.1016/S1567-1356(02)00081-8.
[8] A.J. Cooper, J.T. Pinto, P.S. Callery, Reversible and irreversible protein glutathionylation: biological and clinical aspects, Expert Opin. Drug Metab. Toxicol. 7 (7) (2011) 891–910, https://doi.org/10.1517/17425255.2011.577738.
[9] E.W. Trotter, C.M. Grant, Thioredoxins are required for protection against a reductive stress in the yeast Saccharomyces cerevisiae, Mol. Biol. (N.Y.) 46 (3) (2002) 869–878.
[10] J.R. Pedrajas, B. McDonagh, F. Hernández-Torres, A. Miranda-Vizuete, R. González-Ojeda, E. Martínez-Galisteo, C.A. Padilla, J.A. Bárcena, Glutathione is the resolving thiol for thioredoxin peroxidase activity of 1-cys peroxiredoxin without being consumed during the catalytic cycle, Antioxid. Redox Signal. 24 (3) (2016) 115–128. 10.1089/ars.2015.6366.
[11] L.I. Bruijn, T.M. Miller, D.W. Cleveland, Unraveling the mechanisms involved in motor neuron degeneration in Als, Annu. Rev. Neurosci. 27 (1) (2004) 723–749, https://doi.org/10.1146/annurev.neuro.27.070203.144244.
[12] M. Ghasemi, R.H. Brown, Genetics of amyotrophic lateral sclerosis, Cold Spring Harb. Perspect. Med. 8 (2018), a024125.
[13] J. Wang, A. Caruano-Yzermans, A. Rodriguez, J.P. Scheurmann, H.H. Slunt, X. Cao, J. Gitlin, J.P. Hart, R Borchelt, Disease-associated Mutations at Copper Ligand Histidine Residues of Superoxide Dismutase 1 Diminish the Binding of Copper and Compromise Dimer Stability, J. Biol. Chem. 281 (1) (2007) 345–352, https://doi.org/10.1074/jbc.M604503200.
[14] D. Martins, A.M. English, SOD1 oxidation and formation of soluble aggregates in yeast: relevance to sporadic ALS development, Redox Biol. 2 (2014) 632–639, https://doi.org/10.1016/j.redox.2014.03.005.
[15] R.L. Redler, K.C. Wilcox, E.A. Proctor, L. Fee, M. Caplow, N.V. Dokholyan, Glutathionylation at Cys-111 induces dissociation of wild type and FALS mutant SOD1 dimers, Biochemistry 50 (32) (2011) 7057–7066, https://doi.org/10.1021/bi200614y.
[16] C. Álvarez-Zaldiernas, J. Lu, Y. Zheng, H. Yang, J. Blasi, C. Solsona, A. Holmgren, Cellular redox systems impact the aggregation of cu, zn superoxide dismutase linked to familial amyotrophicn lateral sclerosis, J. Biol. Chem. 291 (33) (2016) 17197–17208, https://doi.org/10.1074/jbc.M115.708230.
[17] M.J. Hitchler, F.E. Domann, Regulation of CuZnSOD and its redox signaling potential: implications for amyotrophic lateral sclerosis, Antioxid. Redox Signal. 20 (10) (2014) 1590–1598, https://doi.org/10.1089/ars.2013.5385.
[18] A.R. Reddi, V.C Culotta, SOD1 integrates signals from oxygen and glucose to repress respiration, Cell 152 (1–2) (2013) 224–235, https://doi.org/10.1016/j.cell.2012.11.046.
[19] C.K.wan Tsang, Y. Liu, J. Thomas, Y. Zhang, X.F.S. Zheng, Superoxide dismutase 1 acts as a nuclear transcription factor to regulate oxidative stress resistance, Nat. Commun. 5 (2014) 3446, https://doi.org/10.1038/ncomms4446.
[20] A. Franceschini, D. Szklarczyk, S. Frankild, M. Kuhn, M. Simonovic, A. Roth, J. Lin, P. Minguez, P. Bork, C.von Mering, L.J. Jensen, STRING v9.1: protein-protein interaction networks, with increased coverage and integration, Nucleic Acids Res. 41 (November 2012) (2013) 808–815, https://doi.org/10.1093/nar/gks1094.
[21] M. Molin, J. Yang, S. Hanzén, M.B. Toledano, J. Labarre, T. Nyström, Life span extension and H2O2 resistance elicited by caloric restriction require the

peroxiredoxin tsa1 in saccharomyces cerevisiae, Mol. Cell 43 (5) (2011) 823–833, https://doi.org/10.1016/j.molcel.2011.07.027.
[22] B. McDonagh, S. Ogueta, G. Lasarte, C.A. Padilla, J.A. Bárcena, Shotgun redox proteomics identifies specifically modified cysteines in key metabolic enzymes under oxidative stress in Saccharomyces cerevisiae, J. Proteomics 72 (4) (2009) 677–689, https://doi.org/10.1016/j.jprot.2009.01.023.
[23] B. McDonagh, G.K. Sakellariou, N.T. Smith, P. Brownridge, M.J. Jackson, Differential cysteine labeling and global label-free proteomics reveals an altered metabolic state in skeletal muscle aging, J. Proteome Res. 13 (11) (2014) 5008–5021, https://doi.org/10.1021/pr5006394.
[24] F. Arnesano, L. Banci, I. Bertini, M. Martinelli, Y. Furukawa, T.V. OHalloran, The unusually stable quaternary structure of human Cu, Zn- superoxide dismutase 1 is controlled by both metal occupancy and disulfide status, J. Biol. Chem. 279 (46) (2004) 47998–48003, https://doi.org/10.1074/jbc.M406021200.
[25] E. Gamero-sandemetrio, R. Gómez-pastor, E. Matallana, Zymogram profiling of superoxide dismutase and catalase activities allows Saccharomyces and non-Saccharomyces species differentiation and correlates to their fermentation performance, Appl. Microb. Cell Physiol. 97 (2013) 4563–4576, https://doi.org/10.1007/s00253-012-4672-1.
[26] X. Chen, H. Shang, X. Qiu, N. Fujiwara, L. Cui, X.M. Li, T.M. Gao, J. Kong, Oxidative modification of cysteine 111 promotes disulfide bond-independent aggregation of SOD1, Neurochem. Res. 7 (4) (2012) 835–845, https://doi.org/10.1007/s11064-011-0679-8.
[27] S. Nitesh, G.K. Tranmer, Hydrogen Peroxide and Amyotrophic Lateral Sclerosis: from Biochemistry to Pathophysiology, Antioxidant 11 (1) (2021) 52, https://doi.org/10.3390/antiox11010052 (Basel).
[28] C. Picazo, H. Orozco, E. Matallana, A. Aranda, Interplay among Gcn5, Sch9 and mitochondria during chronological aging of wine yeast is dependent on growth conditions, PLoS One 10 (2) (2015), https://doi.org/10.1371/journal.pone.0117267.
[29] P. Fabrizio, V.D. Longo, The chronological life span of Saccharomyces cerevisiae, Aging Cell 2 (2) (2003) 73–81, https://doi.org/10.1046/j.1474-9728.2003.00033.x.
[30] C. Picazo, E. Matallana, A. Aranda, Yeast thioredoxin reductase Trr1p controls TORC1-regulated processes, Sci. Rep. 8 (1) (2018), https://doi.org/10.1038/s41598-018-34908-4.
[31] C. Picazo, B. McDonagh, J. Peinado, J.A. Bárcena, E. Matallana, A. Aranda, Saccharomyces cerevisiae cytosolic thioredoxins control glycolysis, lipid metabolism, and protein biosynthesis under wine-making conditions, Appl. Environ. Microbiol. 85 (7) (2019), https://doi.org/10.1128/AEM.02953-18.
[32] M. Canizal-García, B.E. Olmos-Orizaba, M. Moreno-Jiménez, E. Calderón-Cortés, A. Saavedra-Molina, C. Cortés-Rojo, Glutathione peroxidase 2 (Gpx2) preserves mitochondrial function and decreases ROS levels in chronologically aged yeast, Free Radic. Res. 55 (2) (2021) 165–175, https://doi.org/10.1080/10715762.2021.1882677.
[33] F. Roger, C. Picazo, C. Asami, W. Reiter, S. Hanzén, C. Gao, G. Lagniel, N. Welkenhuysen, J. Labarre, T. Nyström, M. Grøtli, M. Hartl, M. Molin, Peroxiredoxin promotes longevity and H2O2-resistance in yeast through redox-modulation of protein kinase a, eLife (2020) 1–32, https://doi.org/10.7554/eLife.60346.
[34] A.F. Tucci, Feedback inhibition of lysine biosynthesis in yeast, J. Bacterioloy 99 (2) (1969) 624–625, https://doi.org/10.1128/jb.99.2.624-625.1969.
[35] R. Gómez-Pastor, R. Pérez-Torrado, E. Cabiscol, J. Ros, E. Matallana, Reduction of oxidative cellular damage by overexpression of the thioredoxin TRX2 gene improves yield and quality of wine yeast dry active biomass, Microb. Cell Fact. 9 (2010) 9, https://doi.org/10.1186/1475-2859-9-9.
[36] R. Gómez-pastor, R. Pérez-torrado, E. Cabiscol, J. Ros, E. Matallana, Engineered Trx2p industrial yeast strain protects glycolysis and fermentation proteins from oxidative carbonylation during biomass propagation, Microb. Cell Fact. 11 (1) (2012) 4, https://doi.org/10.1186/1475-2859-11-4.
[37] R. Gómez-pastor, R. Pérez-torrado, E. Matallana, Modification of the TRX2 gene dose in Saccharomyces cerevisiae affects hexokinase 2 gene regulation during wine yeast biomass production, Appl. Microbiol. Biotechnol. 94 (2012) 773–787, https://doi.org/10.1007/s00253-011-3738-9.
[38] A. Krüger, N.M. Grüning, M.M.C. Wamelink, M. Kerick, A. Kirpy, D. Parkhomchuk, K. Bluemlein, M.R. Schweiger, A. Soldatov, H. Lehrach, C. Jakobs, M. Ralser, The pentose phosphate pathway is a metabolic redox sensor and regulates transcription during the antioxidant response, Antioxid. Redox Signal. 15 (2) (2011) 311–324, https://doi.org/10.1089/ars.2010.3797.
[39] M.A. Sirover, The role of posttranslational modification in moonlighting glyceraldehyde-3-phosphate dehydrogenase structure and function, Amino Acids 53 (4) (2021) 507–515, https://doi.org/10.1007/s00726-021-02959-z.
[40] M. Ralser, M.M. Wamelink, A. Kowald, B. Gerisch, G. Heeren, E.A. Struys, E. Klipp, C. Jakobs, M.l. Breitenbach, H. Lehrach, S. Krobitsch, Dynamic rerouting of the carbohydrate flux is key to counteracting oxidative stress, J. Biol. 6(4) (2007) 10, doi:10.1186/jbiol61.
[41] A.K. Påhlman, K. Granath, R. Ansell, S. Hohmann, L. Adler, The yeast glycerol 3-phosphatases Gpp1p and Gpp2p are required for glycerol biosynthesis and differentially involved in the cellular responses to osmotic, anaerobic, and oxidative stress, J. Biol. Chem. 276 (5) (2001) 3555–3563, https://doi.org/10.1074/jbc.M007164200.
[42] M.E. Walker, J.M. Gardner, A. Vystavelova, C. McBryde, M.D.B. Lopes, V. Jiranek, Application of the reuseable, KanMX selectable marker to industrial yeast: construction and evaluation of heterothallic wine strains of Saccharomyces cerevisiae, possessing minimal foreign DNA sequences, FEMS Yeast Res. 4 (3) (2003) 339–347, https://doi.org/10.1016/S1567-1356(03)00161-2.
[43] U. Güldener, S. Heck, T. Fiedler, J. Beinhauer, J.H. Hegemann, J. Gießen, F. Straße, A new efficient gene disruption cassette for repeated use in budding yeast, Nucleic. Acids. Res. 24 (13) (1996) 2519–2524.
[44] D. Delneri, G.C. Tomlin, J.L. Wixon, A. Hutter, M. Sefton, E.J. Louis, S.G. Oliver, Exploring redundancy in the yeast genome: an improved strategy for use of the cre-loxP system, Gene 252 (1–2) (2000) 127–135.
[45] M.S. Longtine, A. McKenzie, D.J. Demarini, N.G. Shah, A. Wach, A. Brachat, P. Philippsen, J.R. Pringle, Additional modules for versatile and economical PCR-based gene deletion and modification in Saccharomyces cerevisiae, Yeast 14 (10) (1998) 953–961, https://doi.org/10.1002/(SICI)1097-0061(199807)14:10<953::AID-YEA293>3.0.CO;2-U.
[46] A. Adams, C. Kaiser, Methods in Yeast genetics : a Cold Spring Harbor Laboratory Course Manual, Cold Spring Harbor Laboratory Press, Plainview, N.Y, 1998.
[47] V. Garrigós, C. Picazo, E. Matallana, A. Aranda, Wine yeast peroxiredoxin tsa1 plays a role in growth, stress response and trehalose metabolism in biomass propagation, Microorganisms 8 (10) (2020) 1–18, https://doi.org/10.3390/microorganisms8101537.
[48] W. Griffith, Determination of Glutathione and Glutathione Disulfide Glutathione Reductase and 2-Vinylpyridine Using, Anal. Biochem. 212 (1980) 207–212.
[49] C.M. Grant, G. Perrone, I.W. Dawes, Glutathione and catalase provide overlapping defenses for protection against hydrogen peroxide in the yeast saccharomyces cerevisiae, Biochem. Biophys. Res. Commun. 253 (1998) 893–898.
[50] B. Maclean, D.M. Tomazela, N. Shulman, M. Chambers, G.L. Finney, B. Frewen, R. Kern, D.L. Tabb, D.C. Liebler, M.J. Maccoss, Skyline : an open source document editor for creating and analyzing targeted proteomics experiments, Bioinformatics 26 (7) (2010) 966–968, https://doi.org/10.1093/bioinformatics/btq054.
[51] E.E. Luk, V.C. Culotta, Manganese superoxide dismutase in saccharomyces cerevisiae acquires its metal co-factor through a pathway involving the nramp metal transporter, Smf2p *, J. Biol. Chem. 276 (50) (2001) 47556–47562, https://doi.org/10.1074/jbc.M108923200.
[52] W. Jakubowski, T. Bilinski, G. Bartosz, Oxidative stress during aging of stationary cultures of the yeast Saccharomyces cerevisiae, Free Rad. Biol. Med. 28 (2000) 659–664, a.

Further reading

[1] K. Bodvard, K. Peeters, F. Roger, N. Romanov, A. Igbaria, N. Welkenhuysen, G. Palais, W. Reiter, M.B. Toledano, M. Käll, M. Molin, Light-sensing via hydrogen peroxide and a peroxiredoxin Nat, Commun (2017) 14791.
[2] S. Hanzén, K. Vielfort, J. Yang, F. Roger, V. Andersson, S. Zamarbide-Fors, R. Andersson, L. Malm, G. Palais, B. Biteau, B. Liu, M.B. Toledano, M. Molin, T. Nyström, Lifespan control by redox-dependent recruitment of chaperones to misfolded proteins, Cell (2016) 140–151.
[3] Hough M.A., Günter Grossmann J., Antonyuk S.V., Strange R.W., Doucette P.A., Rodriguez J.A., Whitson L.J., John Hart P., Hayward L.J., Selverstone Valentine J., Samar Hasnain S., Dimer destabilization in superoxide dismutase may result in disease-causing properties: structures of motor neuron disease mutants Proc. Natl. Acad. Sci. USA 2004 5976-5981.
[4] Y. Xiong, J.D. Uys, K.D. Tew, D.M. Townsend, S-glutathionylation: from molecular mechanisms to health outcomes Antioxid, Redox Signal (2011) 233–270.